JOURNAL OF MAGNETIC RESONANCE IMAGING 20:684–689 (2004)

Original Research

An Accurate and Robust Method for Unsupervised Assessment of Abdominal Fat by MRI

Vincenzo Positano, MSc,[1]* Amalia Gastaldelli, PhD,[1] Anna maria Sironi, MD,[1] Maria Filomena Santarelli, PhD,[1] Massimo Lombardi, MD,[1] and Luigi Landini, PhD[2]

Purpose: To describe and evaluate an automatic and unsupervised method for assessing the quantity and distribution of abdominal adipose tissue by MRI.

Material and Methods: A total of 20 patients underwent whole-abdomen MRI. A total of 32 transverse T1-weighted images were acquired from each subject. The data collected were transferred to a dedicated workstation and analyzed by both our unsupervised method and a manual procedure. The proposed methodology allows the automatic processing of MRI axial images, segmenting the adipose tissue by fuzzy clustering approach. The use of an active contour algorithm on image masks provided by the fuzzy clustering algorithm allows the separation of subcutaneous fat from visceral fat. Finally, an automated procedure based on automatic image histogram analysis identifies the visceral fat.

Results: The accuracy, reproducibility, and speed of our automatic method were compared with the state-of-the-art manual approach. The unsupervised analysis correlated well with the manual analysis, and was significantly faster than manual tracing. Moreover, the unsupervised method was not affected by intraobserver and interobserver variability.

Conclusion: The results obtained demonstrate that the proposed method can provide the volume of subcutaneous adipose tissue, visceral adipose tissue, global adipose tissue, and the ratio between subcutaneous and visceral fat in an unsupervised and effective manner.

Key Words: abdomen, MR studies; visceral fat; abdominal fat; fuzzy clustering; image processing.
J. Magn. Reson. Imaging 2004;20:684–689.

OBESITY HAS BEEN RECOGNIZED as a risk factor for several chronic diseases, such as non–insulin-dependent diabetes mellitus, dyslipidemia, hypertension, atherosclerosis, and cardiovascular disease in humans (1–3). In particular, the excess accumulation of intra-abdominal adipose tissue seems to be associated with metabolic disorders in obesity. High levels of visceral adipose tissue (VAT) have been linked to an increased risk of obesity-related illnesses, such as diabetes (4).

Measuring the fat quantity and distribution in humans is generally difficult and imprecise. It is especially difficult to characterize the volume and distribution of visceral adipose tissue around the internal organs. Yet to date, there is no simple and reliable method to measure VAT (5). MRI may provide a method to measure adipose tissue safely and accurately. It does not require water submersion or radiation exposure, it can be done rapidly, it provides images that are also useful for clinical diagnosis, and it has been used to characterize adipose tissue volumes (6–8). However, previous MRI methods were either laborious, subject to inter- and intraobserver variability, or limited to the analysis of two-dimensional data.

The first kind of method for fat distribution evaluation in MRI uses the definition of a threshold value that identifies the fat related signal (9). As noted by Elbers et al (10), in MRI fat gives the highest signal intensity, but its absolute intensity varies from image to image and from individual to individual. Therefore, the upper and lower intensity thresholds have to be set separately for each image in order to include the entire adipose tissue area. Gronemeyer et al (8) proposed a fast methodology based on manual image processing of only one representative slice (i.e., the one at the umbilicus level) using Adobe PhotoShop software. They showed that the VAT/subcutaneous adipose tissue (SAT) ratio manually measured on the one slice is strongly correlated with the one measured on all data, although statistical tests show that the fat pixel count was significantly different. The analysis of the image at the umbilicus level is based on a manual choice of a threshold signal intensity value using only a SAT signal. The method is acceptably precise, with an intraobserver variability of 0.2% for SAT and 10.8% for VAT, while interobserver variability is not provided. The most accurate way to measure abdominal fat distribution is the one proposed by Lancaster et al (11). In this approach, the operator defines three contours (external SAT, internal SAT, and a region as small as possible that contains all the VAT). A histogram of the third region is provided and the operator

[1]Institute of Clinical Physiology, CNR, Pisa, Italy.
[2]Department of Information Engineering, University of Pisa, Pisa, Italy.
*Address reprint requests to: V.P., Institute of Clinical Physiology, Consiglio Nazionale Delle Ricerche (CNR), Via Moruzzi, 1 Loc San Cataldo, 56124, Pisa, Italy.
E-mail: positano@ifc.cnr.it
Received November 17, 2003; Accepted June 23, 2004.
DOI 10.1002/jmri.20167
Published online in Wiley InterScience (www.interscience.wiley.com).

manually determines the VAT extension, fitting the second peak of the histogram distribution with a Gaussian curve. This method was recognized as being the best for VAT assessments because it reduces the effects of volume averaging, while using a more natural division between fat and nonfat data. Moreover, the use of histogram classification means that VAT does not have to be manually delimited, which is a difficult task because of the complex structure of the viscera. The approach of Lancaster et al (11) seems to be the one that is generally accepted by the MRI community for assessing abdominal FAT distribution in both humans (10,12,13) and animals (14). However, manual or semiautomatic definition of the three regions is time-consuming and affected by user-related variability, as well as by the manual fitting of histogram fat peak. In this study, we propose an automatic and unsupervised methodology that allows three-dimensional datasets to be processed in a short time without any user interaction. We will show that our unsupervised analysis is significantly correlated with manual analysis, and provides an effective three-dimensional assessment of abdominal fat distribution. Moreover, because the proposed method does not require any user interaction, it is inherently free from any intra- and interobserver variability.

MATERIALS AND METHODS

MRI Protocol

A total of 20 obese and nonobese subjects underwent whole-abdomen MRI. Informed consent was obtained from all subjects. Subjects were imaged on a GE Signa Horizon LX System 1.5-T scanner using a standard body coil with a T1-weighted fast gradient-echo (GE FIESTA) pulse sequence (TR = 120 msec, TE = 4.2 msec, flip angle = 90°, number of excitations [NEX] = 1). A total of 32 images were acquired from each subject in two interleaved sets of 16 images each. The use of the FIESTA sequence allows performing the acquisition in a very short time (about 20 seconds for each set) using the breath-hold technique, avoiding breathing induced motion artifacts. The slice thickness was adapted to patient size in order to cover all abdominal adipose tissue, from the diaphragm to the pelvic region. The field of view ranged from 36 to 48 cm, depending on patient size. The size of the image was 256×256 pixels. The images acquired were retrieved from the MR scanner using the DICOM (Digital Imaging and Communications in Medicine) protocol, and analyzed with custom written homemade software developed in the IDL 6.0 environment. The software is available on request.

Fuzzy C-Mean Cluster Segmentation

The fuzzy c-mean (FCM) approach (15,16) is able to make unsupervised classification of data in a number of clusters, by identifying different tissues in an image without the use of an explicit threshold. The FCM algorithm performs a classification of image data by computing a measure of membership, called fuzzy membership, at each pixel for a specified number of classes. The fuzzy membership function, constrained to be between 0 and 1, reflects the level of similarity between the image pixel at that location and the prototypical data value or centroid of its class. Thus, a membership value near unity means that the image pixel is close to the centroid for that particular class. FCM is formulated as the minimization of the following objective function with respect to the membership function u and centroids v:

$$J_{FCM} = \sum_{j\in\Omega}\sum_{k=1}^{C} u_{jk}^{q} \, \|y_j - v_k\|^2$$

where Ω represents the pixel location in image domain, q is a parameter greater than 1 that determines the amount of fuzziness of the classification ($q = 2$ in our application), u_{jk} is the membership value at location j for class k, y_j is the intensity value at the j-th location, v_k is the centroid of the class k, and C is the number of classes.

When the above objective function is minimized, the value of u_{jk} approaches 1 only if the pixel intensity at j-th location is close to the centroids of class k. Similarly, the value of u_{jk} approaches 0 only if the pixel intensity at the j-th location is far from the centroids of class k. Also, the pixels with the same intensity value are grouped into the same groups with the same probability.

The minimization of J_{FCM} is based on suitably selecting u and v by using an iterative process through the following equations:

$$u_{jk} = \left(\sum_{i=1}^{C} \left(\frac{\|y_j - v_k\|^2}{\|y_i - v_k\|^2} \right)^{\frac{2}{q-1}} \right)^{-1}$$

$$v_k = \frac{\sum_{j\in\Omega} u_{jk}^{q} y_j}{\sum_{j\in\Omega} u_{jk}^{q}}$$

The algorithm stops when the value of u_{jk} converges.

The results of the algorithm are the intensity values that characterize the tissue classes (v_k), and the u_k masks that describe the distribution of the classified tissues along the processed image.

Visceral Fat Analysis

In our problem, three tissue classes can be identified: background/air signal, fat signal, and signal related to other tissues such as muscle, blood, etc. Consequently, we imposed that $C = 3$ in the FCM algorithm. Three masks were extracted from each image, each related to a tissue distribution and to a representative value v_k for the extracted tissues. Figure 1 shows a typical example of masks extracted from an MR image. In each mask, white pixels represent pixels with a high value of u_k (i.e., values near 1.0), dark pixels are related to low values of u_k (i.e., values near 0.0). In other words, white pixels represent the background/air area in Fig. 1b, nonfat tissues in Fig. 1c, and fat tissue in Fig. 1d. Only background/air (u_1) and fat (u_3) maps are used in our meth-

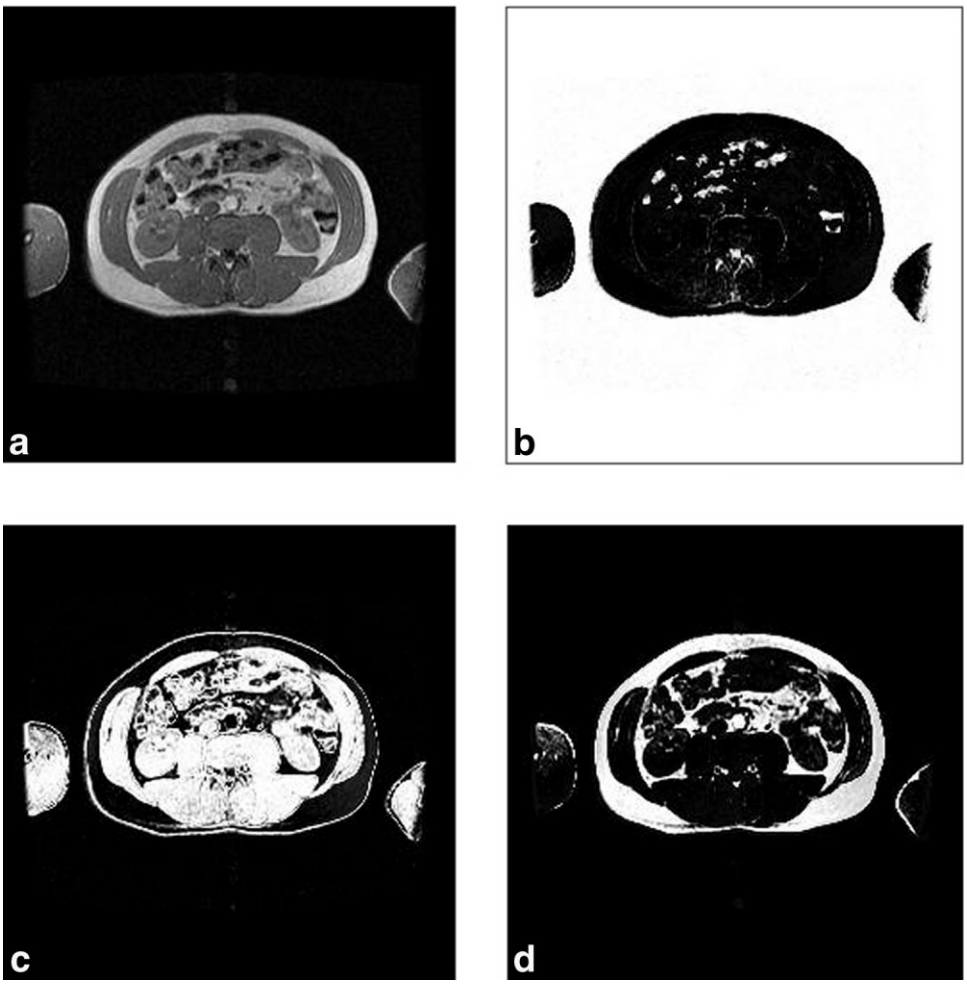

Figure 1. Original image (**a**) and extracted masks for background/air signal (**b**), muscular tissue (**c**) and fat (**d**).

odology. The representative intensity values are v_1 (air), v_2 (nonfat tissue), and v_3 (fat tissue).

The first step consists of automatically cutting patterns of arms on the acquired images, which have to be excluded from the analysis. This is accomplished by automatically selecting a pixel in the center of the image and looking for a pixel with a value near 0 in the u_1 mask. A region-growing algorithm can now easily find all nonbackground pixels in the abdominal region, excluding arms pixels that are not connected with the abdomen.

The mask obtained from the previous step is used to filter the u_3 map, as shown in Fig. 2a. A contour surrounding the abdominal region is automatically created and an active contour algorithm (17) is used to define the external contour of SAT (Fig. 2b). A new contour is defined by cloning the previous one, and the same active contour algorithm is used to find the internal SAT limit (Fig. 2c). Some constraints are included in the active contour algorithm in order to preserve the continuity of the internal SAT contour, thus avoiding erroneous extension in the VAT region. The SAT extension can be now calculated by measuring the area included between internal and external SAT contours. A third contour is now defined by cloning the external SAT contour, and the active contour algorithm is used to limit a region as small as possible that will contain all the VAT signal (Fig. 2d). VAT extension is assessed by automating the methodology suggested by Lancaster et al (11). A Gaussian curve is defined, with a mean value equal to the representative fat value, and a height defined as the number of pixels with a value equal to v_3.

In order to find the standard deviation of the Gaussian curve, we assume that image intensity values higher than v_3 are only related to the fat signal. The Gaussian curve width can be determined by finding the best fit with the histogram curve to the right of the v_3 value, as shown in Fig. 2e. The VAT extension is calculated by evaluating the area of the Gaussian curve.

The results obtained are expressed in terms of numbers of pixels. They can be converted into an area measure (cm^2) by taking into account the pixel size, or in volume measure (cm^3) by taking into account both the pixel size and the slice thickness.

The procedure described can be repeated on all the acquired slices, thus providing an overall assessment of SAT and VAT extension over the entire abdomen, as well as the value of the VAT/SAT ratio.

RESULTS

The proposed method is completely unsupervised, thus no user input is required. This avoids any inter-

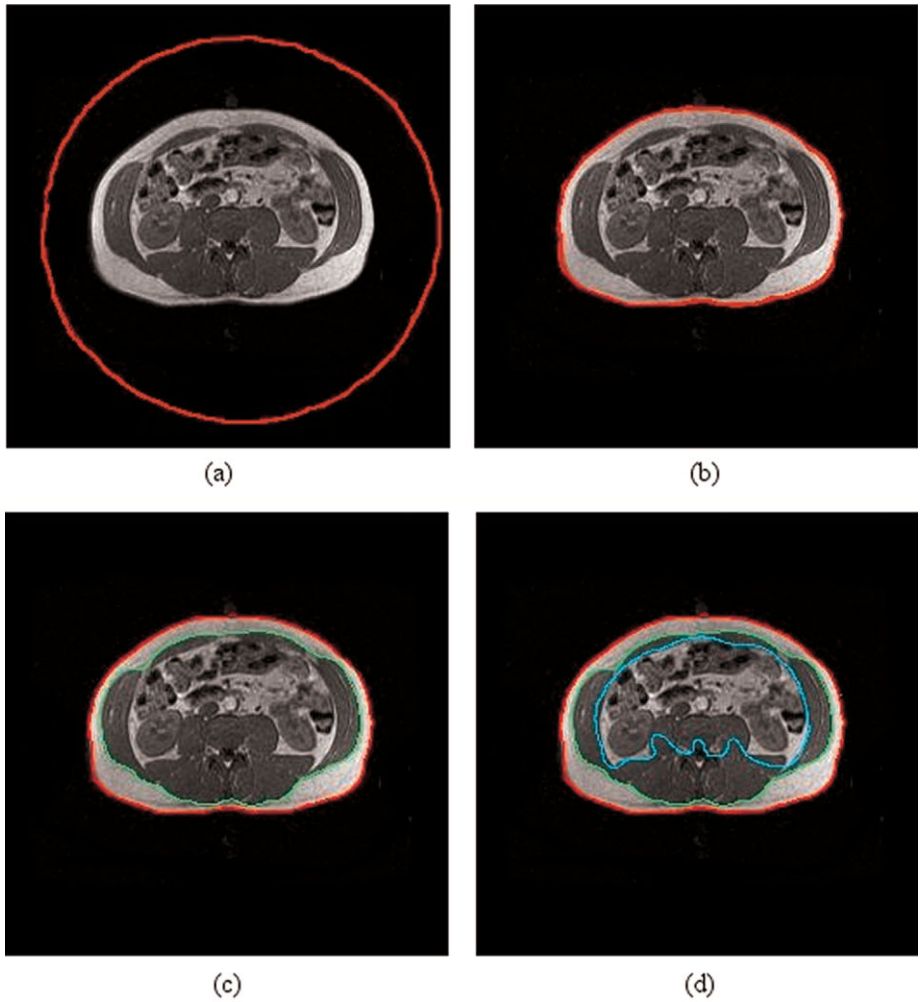

Figure 2. Main phases of subcutaneous and visceral fat detection. **a:** Arms erasing and initial external SAT definition. **b:** External contour of SAT detection. **c:** Internal contour of SAT detection. **d:** VAT area detection. **e:** Automatic analysis of VAT distribution by second peak of image intensity histogram fitted by a Gaussian curve.

or intraobserver variability and ensures that the method is robust. In order to measure the effectiveness of the method, data acquired were compared to that of the classical methodology proposed by Lancaster et al (11) using a trained operator. The latter method entails manually segmenting the SAT, and assessing the VAT by manually defining a rough region containing all VAT signal (Fig. 3). SAT extension

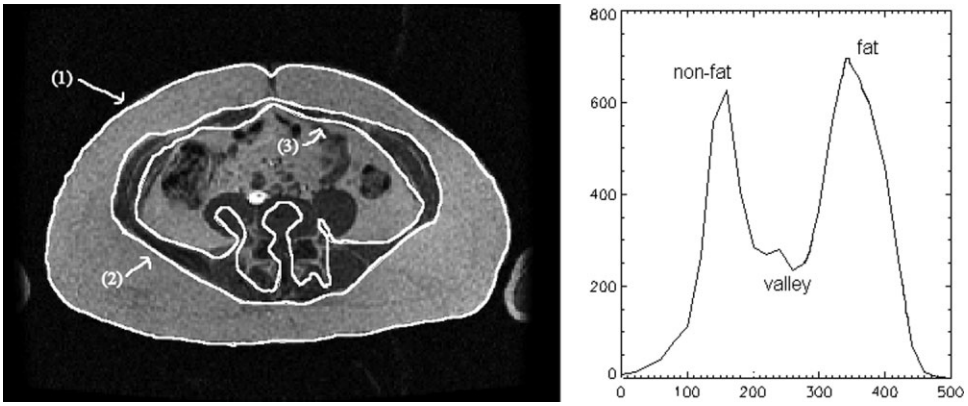

Figure 3. Classical approach for SAT/VAT assessment. Three contours (1 = external contour of SAT, 2 = internal contour of SAT, 3 = VAT area) are required for the manual analysis, together with the analysis of the histogram of the fat peak of the region (3).

is considered to be the area between the external and internal SAT contours. The VAT is assessed by inspecting the histogram extracted from the third region, which will contain both VAT and other tissues. The histogram has two peaks, and the right-hand one is related to VAT distribution. A threshold is manually defined in the valley region, and the VAT area is assessed by integrating the histogram curve above this threshold pixel value. It is important to note that this methodology can fail when the extension of VAT is small because the VAT-related peak could be passed by the non-VAT-related one. Moreover, the fitting of the VAT peak with the Gaussian curve can be affected by intra- and interoperator variability.

A total of 640 images (20 patients, 32 images each) were processed with both the manual and the unsupervised methods. The overall extension of SAT and VAT for each patient was then evaluated with both methods. With regard to the overall assessment of VAT and SAT on all 20 subjects, the correlation between unsupervised and manual approaches is very high for both SAT ($r = 0.9917$, $P < 0.0001$) and VAT ($r = 0.9601$, $P < 0.0001$) assessments. Figure 4 shows the Bland-Altman plot for subcutaneous fat assessment on all 20 subjects. The SAT volumes calculated using the unsupervised method were slightly greater than those obtained by the manual method. The unsupervised methodology's overestimation of SAT in some slices is mainly due to erroneous arms erasing, which extends the SAT assessment to the arms tissue. This problem should be avoided at an acquisition level by putting a spacer between the patient's arms and abdomen.

On the other hand, the VAT volumes calculated using the unsupervised methodology were slightly underestimated with respect to the manual method, as shown by the Bland-Altman plot in Fig. 5. Underestimation of VAT tissue seems to be mainly due to the erroneous assessment of VAT distribution in images with a low presence of visceral fat. This result is not surprising, because in the previous condition, the second peak of the histogram used for the VAT assessment may be hidden by the preponderant signal of nonfat tissues. In this case, both manual and unsupervised approaches may lead to incorrect results. Moreover, our approach assumes that the histogram of fat values is symmetric. Partial volume effect can lead to a deformation of the Gaussian histogram related to fat distribution. This effect can leads to a underestimation of the VAT volume.

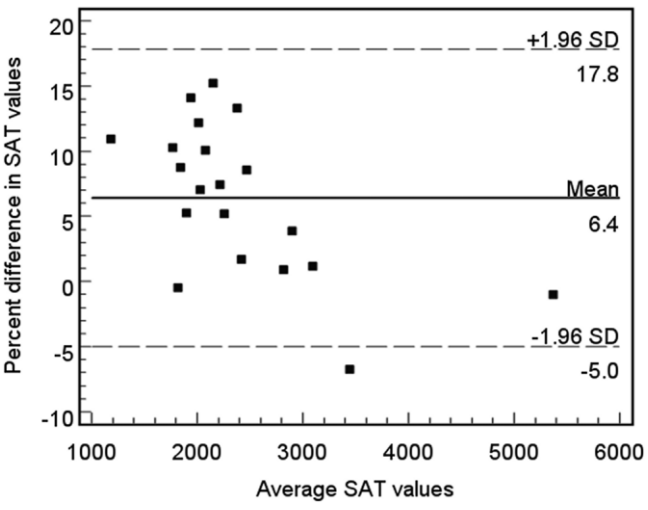

Figure 4. Bland-Altman plot for overall SAT assessment on all 20 subjects.

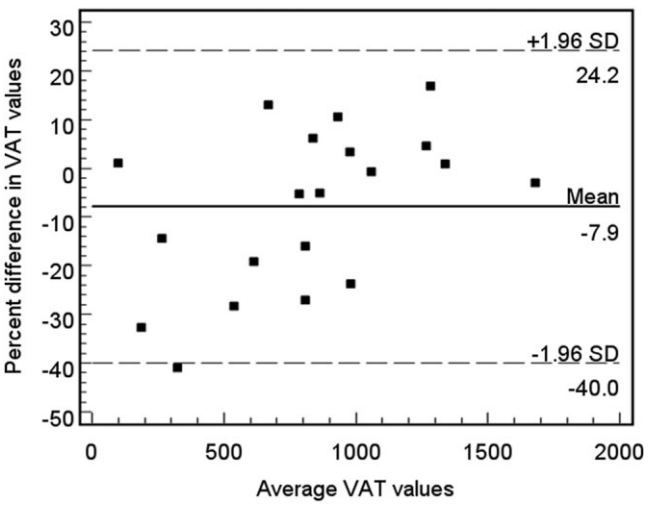

Figure 5. Bland-Altman plot for overall VAT assessment on all 20 subjects.

DISCUSSION

Measuring abdominal fat distribution in MR images is not a simple task. Although measuring subcutaneous fat is quite simple, measuring visceral fat is difficult due to the complex structure of the viscera and the presence of artifacts such as volume averaging, patient movements, and magnetic field inhomogeneities. The most accepted method for accurately assessing VAT distribution entails classifying visceral tissue into two classes: fat and nonfat. This is accomplished using the visceral area histogram and fitting the second peak of the histogram with a Gaussian curve that approximates the distribution of the fat signal. Because the value of the mean fat signal varies from image to image, this approach is time consuming (about one hour for each subject) and requires a manual review of all acquired images. Moreover, for nonobese subjects, the fat signal may be passed by the nonfat one (i.e., the nonfat signal may go over the fat signal) thus manual segmentation of the visceral fat may be required.

Other approaches are based on the choice of intensity threshold that identifies the separation between fat and nonfat tissues (8). The main drawback of this method is the need to manually define a different threshold for each image. Consequently, in order to reduce the time required for data processing, the analysis of abdominal MRI is often limited to only one slice at the umbilicus level. Many authors have shown a good correlation between measurements on one slice and measurements of the whole abdominal volume (8,11). However, three-dimensional analysis can provide real data about fat volumes, and reduces the influence of analysis mistakes by averaging the error effect on a large number of analyzed images.

We propose a methodology that performs three-dimensional unsupervised assessment of abdominal fat distribution. The method does not require any user interaction and consequently is not affected by intra or interobserver variability. Because the analysis is unsupervised, the time required for the analysis does not really matter. However, the processing time (about six minutes) is short enough to allow a real time analysis. The results obtained with the unsupervised method were compared with ones obtained with the state-of-art methodology. The accuracy of the former was excellent both with regard to the measurement of the whole abdominal fat as well as measurement of individual slices.

In conclusion, the proposed methodology is shown to be accurate and robust, and has a significant advantage over manual tracing in terms of speed. This allows three-dimensional analysis of abdominal MRI images to be carried out with minimal user intervention, providing useful clinical indices for the characterization of abdominal fat distribution.

ACKNOWLEDGMENTS

We thank Dr. Brunella Favilli and Dr. Roberta Petz for their help in data acquisition and analysis and the anonymous reviewers for their comments.

REFERENCES

1. Wajchenberg BL. Subcutaneous and visceral adipose tissue: their relation to the metabolic syndrome. Endocr Rev 2000;21:697–738.
2. Mann GV. The influence of obesity in health. [Review Part 1] N Engl J Med 1974;291:178–185. [Review Part 2: 1974;291:226–232]
3. Manson JE, Colditz GA, Stampfer MJ, et al. A prospective study of obesity and risk of coronary hearth disease in women. N Engl J Med 1990;322:882–889.
4. Kitabchi AE, Buffington CK. Body fat distribution, hyperandrogenicity, and health risks. Semin Reprod Endocrinol 1994;12:6–14.
5. Abate N, Burns D, Peshock RM, Garg A, Grundy SM. Estimation of adipose tissue mass by magnetic resonance imaging: validation against dissection in human cadavers. J Lipid Res 1994;35:1490–1496.
6. Gray DS, Fujioka K, Colletti PM, et al. Magnetic resonance imaging used for determining fat distribution in obesity and diabetes. Am J Clin Nutr 1991;54:623–627.
7. Ortiz O, Russel M, Daley TL, et al. Differences in skeletal muscles and bone mineral mass between black and white females and their relevance to estimates of body composition. Am J Clin Nutr 1992; 55:8–13.
8. Gronemeyer SA, Steen RG, Kauffman WM, Reddick E, Glass JO. Fast adipose tissue (FAT) assessment by MRI. Magn Reson Imaging 2000;18:815–818
9. Ross R, Leger L, Morris D, De Guise J, Guardo R. Quantification of adipose tissue by MRI: relationship with anthropometric variables. J Appl Physiol 1992;72:787–795.
10. Elbers JMH, Haumann G, Asscheman H, Seidell JC, Gooren LJG. Reproducibility of fat area measurements in young, non-obese subjects by computerized analysis of magnetic resonance images. Int J Obes Relat Metab Disord 1997;21:1121–1129.
11. Lancaster JL, Ghiatas AA, Alyassin A, Kilcoyne RF, Bonora E, De Fronzo RA. Measurement of abdominal fat with T1-weighted MR images. J Magn Reson Imaging 1991;1:363–369.
12. Gastaldelli A, Miyazaki Y, Pettiti M, et al. Metabolic effects of visceral fat accumulation in type 2 diabetes. J Clin Endocrinol Metab 2002;87:5098–5103.
13. Bonora E. Relationship between regional fat distribution and insulin resistance. Int J Obes Relat Metab Disord 2000;24:S32–S35.
14. Ishikawa M, Koga K. Measurement of abdominal fat by magnetic resonance imaging of OLETF rats, an animal model of NIDDM. Magn Reson Imaging 1998;16:45–53.
15. Udupa JK, Samarasekera S. Fuzzy connectedness and object definition: Theory, algorithm and application in image segmentation. Graph Models Image Process 1996;58:246–261.
16. Bezdek J, Hall L, Clarke L. Review of MR image segmentation using pattern recognition. Med Phys 1993;20:1033–1948.
17. Kass M, Witkin A, Terzopoulos D. Active contours models. Int J Comput Vis 1987;1:321–331.